Microchemical Journal 183 (2022) 108033

Contents lists available at ScienceDirect

Microchemical Journal

journal homepage: www.elsevier.com/locate/microc

Study of the protective role of Zn in cultured retinal pigment epithelial cells subjected to pro-inflammatory conditions using transcriptomics and mass spectrometry

Marta Aranaz [a], Ana Álvarez-Barrios [a,d], Marta Costas-Rodríguez [b,*], Lara Lobo [a,*], Lydia Álvarez [c,d], Héctor González-Iglesias [c,d,e], Rosario Pereiro [a,d], Frank Vanhaecke [b]

[a] Department of Physical and Analytical Chemistry, University of Oviedo, Julián Clavería 8, 33006 Oviedo, Asturias, Spain
[b] Department of Chemistry, Atomic & Mass Spectrometry – A&MS Research Unit, Ghent University, Campus Sterre, Krijgslaan 281 - S12, 9000 Ghent, Belgium
[c] Instituto Oftalmológico Fernández-Vega, Avda. Fernández-Vega 34, 33012 Oviedo, Spain
[d] Instituto Universitario Fernández-Vega, Fundación de Investigación Oftalmológica, Universidad de Oviedo, Spain
[e] Department of Technology and Biotechnology of Dairy Products, Instituto de Productos Lácteos de Asturias, Consejo Superior de Investigaciones Científicas (IPLA-CSIC), Villaviciosa, Spain

ARTICLE INFO

Keywords:
Transcriptomics
Elemental & isotopic analysis
Cell culture
Mass spectrometry
Inflammation processes
Zn supplementation

ABSTRACT

The present work aimed at investigating Zn alterations as a response to an inflammatory process in an *in vitro* human retinal pigment epithelial (RPE) cell model mimicking aging process. Cells were subjected to acute inflammatory stress with and without Zn supplementation and the effects of such exposure were evaluated by studying alterations at the transcriptome level and in the Zn concentration and its isotopic composition using single-collector and multi-collector ICP-mass spectrometry, respectively. The *in vitro* RPE model strongly responded to pro-inflammatory events (caused using 100 U/mL Interleukin-1α) at the RNA level by inducing immune and cytokine responses, while Zn supplementation (100 μM Zn) partially attenuated the aforementioned inflammatory effects. Interestingly, the Zn isotope ratios were correlated with the transcriptome, as inflammation was demonstrated to lead to a lighter Zn isotopic composition. This change in the isotopic composition of Zn signaling inflammation, which could also be avoided by short-term zinc supplementation, is probably indicating the modulation of the cellular immune function via cytokine signaling.

1. Introduction

The retinal pigment epithelium (RPE) is a monolayer of pigmented cells, contributing to the homeostasis of the neurosensory retina by removing by-products of the visual cycle. Retina and RPE aging lead to uncontrolled inflammation, resulting in cell damage, which disrupts its immune-privilege and contributes to the onset of age-related macular degeneration (AMD), an irreversible eye disease [1,2]. Zinc deficiency or excess triggers the development of different neurodegenerative diseases, e.g. Alzheimer, Ischemic stroke or Parkinson [3,4]. Zn also plays an important role in aging-related eye disorders as a regulator of the antioxidant pathway and as an anti-inflammatory agent [5–8]. It has been shown that Zn supplementation reduces AMD progression at intermediate and late stages [9]. Specifically, this essential trace metal, involved in retinal functions such as phototransduction and neurotransmission [10,11], modulates the cellular immune function of *T*-cells via cytokine signalling [12,13].

Zn homeostatic fluctuations are mediated by cytosolic zinc-binding proteins and cell influx and efflux cellular transport mechanisms, involving metallothioneins (MTs) and the two families of zinc transporters, ZnT (Zinc Transporter) involved in its export and ZIP (Zinc Importer), promoting its influx from the extracellular compartment into the cytoplasm [8,14,15]. Both MTs and Zn transporters are expressed by RPE cells, which are altered during aging and disease, suggesting a pathological consequence for the health and function of the retina [5]. Still, the link between Zn and inflammation in the RPE is not well understood and very little is known about the metabolic pathways for Zn transport and its relevance in the physiology and pathophysiology of the eye.

These biochemical mechanisms may be accompanied by isotope

* Corresponding authors.
E-mail addresses: Marta.CostasRodriguez@ugent.be (M. Costas-Rodríguez), lobolara@uniovi.es (L. Lobo).

https://doi.org/10.1016/j.microc.2022.108033
Received 1 July 2022; Received in revised form 27 September 2022; Accepted 28 September 2022
Available online 3 October 2022
0026-265X/© 2022 The Author(s). Published by Elsevier B.V. This is an open access article under the CC BY-NC-ND license (http://creativecommons.org/licenses/by-nc-nd/4.0/).

fractionation effects due to a slightly different behaviour of isotopes of the same element [16]. The heavier isotope(s) of a given element shows/show a preference for the stronger chemical bonds, whereas the lighter isotopes show a higher reaction rate [17]. High-precision isotopic analysis has been demonstrated to be an outstanding tool for identifying changes in metabolic processes, while isotope ratios of essential mineral elements are increasingly suggested as potential biomarkers for early diagnosis of diseases [18–20]. In this context, alterations in the Zn isotopic composition of biological fluids and tissues have been found in glaucoma and cancer; glaucoma patients showed a significantly lighter Zn isotopic composition in their aqueous humor compared to that of healthy subjects [21]. Breast cancer tumour tissue displays a lighter Zn isotopic composition than that of the blood, serum and healthy breast tissue [22]. Also the urine Zn isotopic composition of patients suffering from pancreatic or prostate cancer or from benign breast disease was lighter than that of healthy subjects [23].

The study of isotope fractionation *in vitro* has been shown to provide further insights in the molecular pathways of trace elements under different experimental conditions. In this line, an intestinal Caco-2 cell line was used to experimentally demonstrate isotope fractionation favouring the lighter Fe isotopes during intestinal absorption. After 24 h of exposing the cell line to an Fe-containing solution in a bicameral experiment, the isotopic composition in the apical chamber had become isotopically heavier than at the start, while the basal solution was demonstrated to contain isotopically lighter Fe, evidencing a preferential uptake and transport of the lighter isotopes [24]. In another study using the hepatic cell line HepG2, it was reported that hypoxia induces a heavier cellular Cu isotopic composition [25]. The same trend was observed for the HepG2 cell line under oxidative stress conditions [26]. Conversely, a preferential uptake of the lighter Cu and U isotopes was observed in cultured human neuronal cells (SH-SY5Y) upon exposure to U [27]. Using the same neuronal cell line, it has been shown that cells were systematically enriched in the light ^{63}Cu isotope with increasing intracellular metal content, with the mitochondria being isotopically lighter than the cell lysate [28]. Surprisingly, for the breast cancer MDA-MB-231 cell line, a preferential cellular uptake of the heavier Zn isotopes was observed, *i.e.* Zn isotope fractionation in the opposite direction to that observed for *in vivo* breast cancer tissue. This difference was hypothetically attributed to differences in Zn transporter levels or intercellular Zn storage mechanisms [29].

Research on high-precision isotopic analysis via multi-collector (MC)-ICP-MS in cell cultures is still limited due to analytical challenges, mainly caused by the low amount of analyte available for analysis, and potential contamination, particularly in the context of Zn isotopic analysis. The control of blank levels is crucial to get reliable Zn isotope ratio results for *in vitro* cell cultures.

The main goal of the present investigation was to study Zn alterations as a response to an inflammatory process by using a RPE cell model mimicking aging and inflammatory processes. The experiments performed aim at improving the understanding of the metabolic processes involving Zn and their relevance in the physiology and pathophysiology of neurodegenerative diseases resembling AMD disease. In particular, such aim has been pursued by investigating Zn alterations in response to inflammation and Zn supplementation at three different levels: differential gene expression, Zn concentration and Zn isotopic composition.

2. Material and methods

2.1. Reagents

Ultrapure water was obtained from a Milli-Q Element water purification system (Merck Millipore, USA). Trace metal analysis grade 14 M HNO_3 (Fisher Chemicals, UK) and 12 M HCl (Fisher Chemicals, UK) were used throughout this work, after further purification by sub-boiling distillation in a PFA purification system (Savillex Corporation, USA). Ultrapure TraceSELECT® 9.8 M H_2O_2, used for sample digestion and isolation of the target element, was purchased from Sigma Aldrich (Belgium). Polypropylene chromatographic columns and AG® MP-1 resin (100–200 mesh, chloride form, Bio-Rad, Belgium) were used for Zn isolation from the sample matrix.

Single-element standard stock solutions used for quantification and mass bias correction were purchased from Inorganic Ventures (The Netherlands). The isotopic certified reference material IRMM-3702 (Institute of Reference Materials and Measurements, Belgium) was used for external mass bias correction. A single-element Zn standard solution (Inorganic Ventures, USA), previously characterized for its isotopic composition, was used as in-house isotopic standard for quality assurance/quality control (QA/QC).

For cell culture treatments, zinc sulphate monohydrate was purchased from Sigma-Aldrich (Spain), while pro-inflammatory Interleukin-1 alpha (IL1α) was purchased from GoldBio® (USA).

2.2. Cleaning protocol

The manipulation of the cell cultures was carefully optimized with the aim of avoiding contamination from both an analytical and biological point of view. In this vein, all material (tips and Eppendorf tubes) was previously cleaned with 1.2 M HCl + 0.001 % H_2O_2, rinsed with Milli-Q water and carefully stored after drying. This material was used for sample collection, whereas Zn and IL1α supplementation was carried out with sterilized pipette tips. Before use, this material was also subjected to UV light for 30 min to assure sterilization.

From an analytical point of view, it is well known that proper cleaning with the aim of minimizing Zn contamination is mandatory. For such purpose, cell culture experiments were performed in a laminar flow hood under sterilized conditions at the Fernandez-Vega Ophthalmological Research Foundation (Oviedo, Spain), ensuring maximum control over the Zn blank levels, whereas sample preparation for Zn quantification and isotope ratio measurements was carried out inside a class-10 clean lab (at the A&MS facilities, Ghent University, Belgium). Teflon Savillex® beakers were pre-cleaned with 7 M HNO_3 and 6 M HCl in several steps and the polyethylene material was cleaned with 1.4 M HNO_3 and ultrapure water.

2.3. RPE cell culture

The primary human fetal RPE cells (hfRPE) were commercially obtained from ScienCell Research Laboratories (USA) at passage 1 (*P*1). Cells were propagated and frozen as *P*2 cells. For our experiments, unfrozen cells (*P*3) were seeded at a density of 142,900 cells/cm^2 onto 12-well Transwell® inserts (10 μm thick polyester inserts with 0.4 μm pore size, Corning, Thermo Fisher Scientific, USA), previously coated with Geltrex™ extracellular matrix (Thermo Scientific, USA). The main feature of the Transwell® inserts is the design of a bicameral chamber, which mimics *in vivo* conditions. The 0.4 μm pores in the insert membrane hinder the movement of microparticles between chambers, but nanoparticles released by cells can pass from the upper (apical side) to the lower compartment (basal side). Cultures from three 12-well Transwell® plates were used for the experiments (*i.e.*, Plates 1, 2 and 3). The cells were grown in EpiCM (Epithelial Cell Medium, ScienCell Research Laboratories) supplemented with 2 % fetal bovine serum (FBS), 1 % penicillin–streptomycin and 1 % epithelial cell growth supplement (EpiCGS) and incubated at 37 °C with 5 % CO_2. After seven days, the culture medium was replaced by MEM-α modifications (Minimum Essential Medium Eagle Alpha Modification; Sigma-Aldrich) as previously described [30]. This culture medium, which contributes to the differentiation of the RPE cells, was replaced 2–3 times a week and cellular differentiation was monitored through the observation of the increase of cell pigmentation and the acquisition of cobblestone morphology, evaluated by means of the inverted microscope LEICA DM IL LED (Leica Microsystems). Moreover, the monolayer integrity was regularly checked prior to change of culture medium by measuring the

transepithelial electrical resistance (TEER), using the Minicell ERS-2 Epithelial Volt-Ohm Meter and STX01 electrodes (Millipore Corporation, MA, USA) [30,31].

2.4. Cell experiments

After 31 days, when the cell cultures showed characteristics of a mature RPE, the cells in Plates 1, 2 and 3 were apically incubated for 24 h with either: 1) Miller medium (further referred to as control); 2) 100 U/mL IL1α in Miller medium (further referred to as IL1α-treatment) or 3) 100 μM Zn, prepared from $ZnSO_4{\cdot}H_2O$ (Sigma-Aldrich) in Miller medium (further referred to as Zn-treatment), whereas only Miller medium was added to all the basal compartments (see Fig. 1). Incubation time and concentrations of Zn and IL1α were similar to those used in previous works in corneal, lens and RPE immortalized cell lines [15,32,33]. All incubations were carried out at 37 °C in a humidified atmosphere with 5 % CO_2. After incubation, each plate was processed as follows:

- Plate 1: The apical and basal media from the cultures of Plate 1 were separately collected, the cell cultures were washed three times with Dulbeccós phosphate-buffered saline (DPBS, Sigma Aldrich) and the wash solutions of each culture were also collected. Then, the Plate 1 containing the cells, the apical and the basal media, and wash solutions were stored at −80 °C until elemental and isotopic analysis.
- Plate 2: The apical and basal media from the cultures of Plate 2 were separately collected. Cell cultures of Plate 2 were maintained for an additional 24 h to be incubated in Miller medium with or without supplementation as follows: those cultures previously incubated with 100 U/mL IL1α were supplemented with 100 μM Zn (further referred to as IL1α + Zn-treatment), while those previously incubated with 100 μM Zn were exposed to 100 U/mL IL1α (further referred to as Zn + IL1α-treatment). The rest of the cultures of this plate were incubated with Miller medium only (as controls). After 24 h of incubation, the apical and basal media were separately collected, the cells were washed as previously described, and media, wash solutions and Plate 2 were stored at −80 °C until elemental and isotopic analysis.
- Plate 3, the culture media were removed and RNA was isolated from two untreated cell cultures (control), two IL1α-treated cell cultures (IL1α-treatment) and another two cell cultures incubated with Zn (Zn-treatment). Later, the remaining two cell cultures from Plate 3, incubated previously with 100 μM Zn, were incubated for an additional 24 h with 100 U/mL IL1α (Zn + IL1α-treatment). Then, the culture media were removed and RNA was isolated and stored at −80 °C until analysis.

2.5. RNA isolation and sequencing

The RNA of 8 cell cultures (see Fig. 1) from Plate 3 was extracted with a RNeasy Mini Kit (Qiagen). After removing the culture media, lysis buffer was added to the cells. Subsequently, the lysed cells corresponding to each culture were transferred to RNase-free Eppendorf tubes. RNA isolation was performed according to the manufacturer's protocol. RNA sequencing and bioinformatics analysis were performed at the BGI Corporation (Beijing Genomics Institute, Shenzhen, China), which uses its own Next Generation Sequencing platform, designated as BGISEQ-500. Differential expression between condition groups (Control, Zn-treatment, IL1α-treatment and Zn + IL1α-treatment), each made up of two biological replicates, was conducted using the DESeq2 analysis method [34,35]. Differentially expressed genes (DEGs) were identified with a threshold value for p_{adj} (adjusted p-value) $\leq$ 0.05 and fold-change $\geq$ 2 or $\leq$ 0.5. Gene ontology (GO) enrichment analysis of DEGs was carried out to determine the most significantly enriched biological process terms.

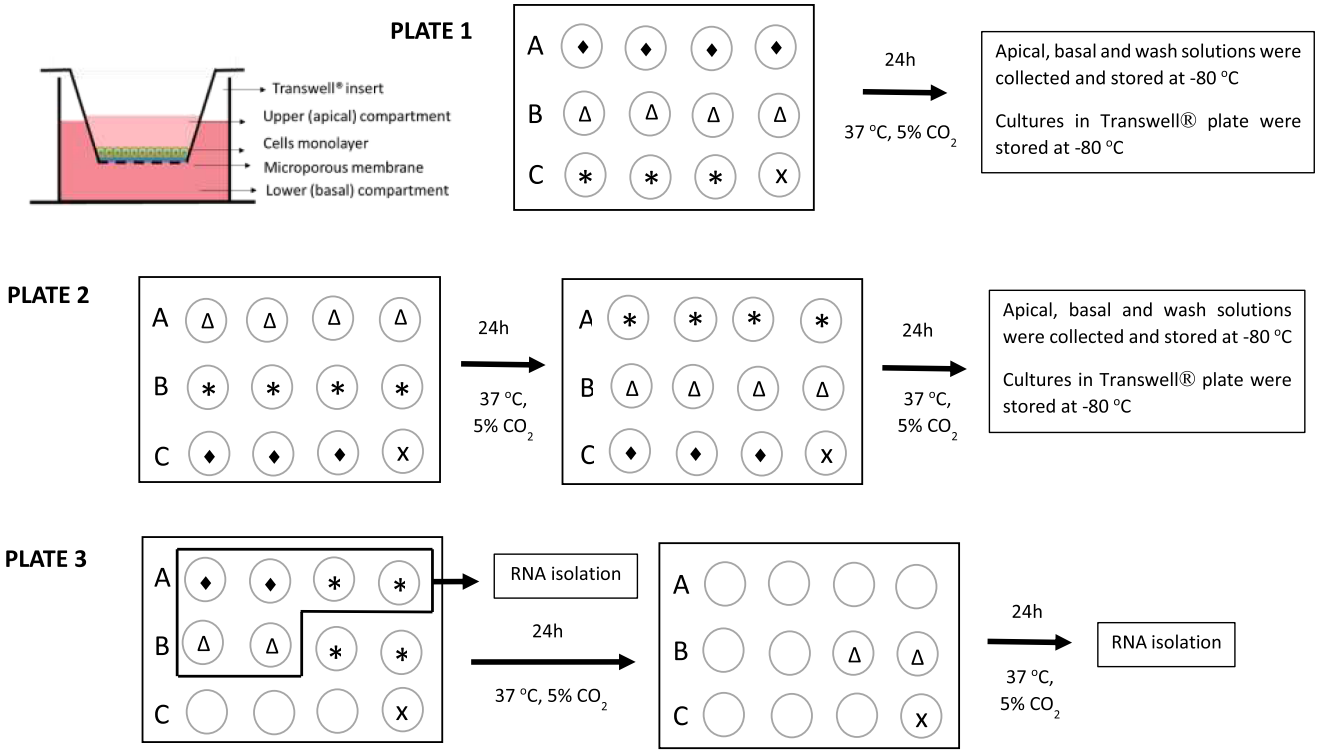

Fig. 1. Experimental design. **Medium in the apical compartment:** ◆ Miller medium added to the control cells; **x** Miller medium added to the Transwell® insert without cells (procedural blank); * 100 μM Zn in Miller medium, **Δ** 100 U/mL IL1α in Miller medium. **Medium in the basal compartment:** Miller medium in all chambers. **x** Transwell® insert without cells (procedural blank).

2.6. Sample preparation for isotopic analysis

Culture media (apical and basal) and wash solutions from each Transwell® (Plates 1 and 2) were acid digested in Teflon Savillex® beakers using a mixture of 3 mL 14 M HNO_3 and 500 μL of 9.8 M H_2O_2 during 18 h at 110 °C. The same procedure was applied for the digestion of the cells from same Plates, although 500 μL of 14 M HNO_3 and 150 μL of 9.8 M H_2O_2 were used instead. For such purpose, the cells were first defrosted and directly removed from the porous membrane by addition of a small amount of 14 M HNO_3 (about 200 μL in two steps) to the Transwell®. The acid was then transferred to Savillex® beakers and digestion accomplished. This procedure (direct freezing of the cell grown on the porous membrane and later removal of the cells using HNO_3) allowed to avoid contamination. It is noteworthy that when cells were collected from the Plate using the conventional trypsinization procedure, reliable isotopic analysis was no longer possible due to Zn contamination.

The digests obtained were evaporated to dryness at 90 °C and, subsequently, reconstituted in 0.5 mL of 8 M HCl. An aliquot of this solution (20 μL) was used for Zn quantification by means of a sector-field inductively coupled plasma-mass spectrometry (using an Element XR instrument, Thermo Scientific, Germany). The Zn concentration obtained was not always sufficient to allow reliable Zn isotopic analysis (in case of a Zn concentration < 100 μg/L in the digest). In such case, sample replicates were combined to obtain a higher amount of Zn. Then, samples were taken up in 5 mL (final volume) of 8 M HCl with 0.001 % H_2O_2. Zn isolation was performed using anion exchange chromatography with 1 mL of AG® MP1 resin (Bio-Rad), as described elsewhere [36]. After isolation, the final solution was dried and reconstituted in 500 μL of 0.28 M HNO_3. An aliquot of 20 μL of this solution further diluted with 0.28 M HNO_3 was used for Zn quantification with the aim of assuring quantitative recovery, assuring that the Zn fraction did not show evidence of on-column isotope fractionation. The rest of the solution was used for Zn isotope ratio measurements. Throughout the entire experiment (digestion and isolation), two procedural blanks were included in each batch of samples for QC purposes.

2.7. Instrumentation and Zn isotope ratio measurements

Zn elemental determination was accomplished using an Element XR single-collector sector-field ICP-MS unit (Thermo Scientific, Germany), operated at medium mass resolution (R = 4,000). The instrument, in operation at Ghent University, was equipped with a 200 μL/min quartz concentric nebulizer and a cyclonic spray chamber for sample introduction. Quantitative Zn determination was performed via external calibration with Ga as an internal standard (10 μg/L) to correct for matrix effects, signal drift and instrumental instability. Elemental determination was accomplished before and after Zn isolation to assure quantitative recovery of the target element.

Zn isotope ratio measurements were performed using a Neptune XT multi-collector (MC)-ICP-MS instrument (Thermo Scientific) equipped with a high transmission Jet interface (Jet-type Ni sampling cone and X-type Ni skimmer cone), also in operation at Ghent University. The sample introduction system consisted of a PFA C-type nebulizer (100 μL/min) and a heated spray chamber, combined with a PTFE membrane desolvator unit (Aridus II unit, Teledyne Cetac Technologies, USA). Measurements were performed at medium (pseudo) mass resolution and the ion beams of interest were monitored using 6 Faraday cups, all connected to 10^{11} Ω amplifiers. Samples were run in a sample-standard bracketing sequence (SSB). The isotopic certified reference material IRMM-3702 (Institute of Reference Materials and Measurements, Belgium) was used as external standard and Cu was added for internal correction according to Baxter *et al.* (revised Russelĺs model) [37]. The solutions (samples and standards) were adjusted to 20 μg/L Zn and 20 μg/L Cu (within ± 3 %) to avoid mass bias variation. For those samples where the Zn concentration was sufficiently high, the Zn isotope ratio measurements were also performed in wet plasma conditions for comparison purposes. In such cases, the measurement solutions were adjusted to 200 μg/L Zn and 200 μg/L Cu in 0.28 M HNO_3 and the sample introduction system consisted of a PFA concentric nebulizer (100 μL/min) mounted onto a tandem spray chamber (with a cyclonic and a Scott-type sub-unit). An in-house standard (previously characterized for its isotopic composition) was measured at the beginning of each measurement sequence and every-five samples for monitoring the quality of the isotopic analysis in both dry and wet plasma conditions.

3. Results and discussion

3.1. Characterization of primary RPE cell cultures

Thirty RPE cell cultures were grown on Transwell® inserts and their maturation in terms of morphology, pigmentation and TEER was followed for 31 days (Fig. 2). Culture conditions under which RPE cells develop characteristics similar to those of mature RPE *in vivo* [38–40] were selected. After 11 days, our cultures developed cobblestone morphology and small groups of pigmented cells were observed; these increased in size and number over time (see Fig. 2a). Additionally, an increase in TEER was observed from day 10 onwards in all cultures, indicating the establishment of tight intercellular junctions, enabling the formation of the epithelium barrier function. Fig. 2b shows the evolution of the average TEER with cell culture time, reaching the maximum value at 31 days, *i.e.* TEER = 103 ± 48 Ohm cm^2. The high standard deviation of the TEER values shows the biological heterogeneity of the cultures. In the native tissue, TEER values reach 150 Ohm cm^2, while securing reproducible TEER values in cellular models of RPE are still a difficult task, although values close to 100 Ohm cm^2 guarantee cell culture formation of single monolayers [30].

Also the gene expression of the matured RPE cells was checked and characteristic gene expression indicated the differentiation aimed at. As shown in Table 1, transcriptome analyses (Plate 3) confirmed that cultured cells expressed genes codifying RPE-specific proteins, including bestrophin-1 (BEST-1), cellular retinaldehyde-binding protein (CRALBP), retinoid isomerohydrolase RPE65 (RPE65) and retinal G protein coupled receptor (RGR), which are all related with the visual cycle, and tyrosinase (TYR), melanocyte inducing transcription factor (MITF) and tyrosinase related protein 1 (TYRP1), which are involved in melanogenesis process.

3.2. Transcriptome analysis and differential gene expression

We studied the effects of exogenously supplemented zinc, in the form of $ZnSO_4$, and/or pro-inflammatory IL1α treatment on hfRPE cells, by determining their entire transcriptomic profile, along with specific changes in the gene expression of metallothioneins (MTs) and cytokines [32] as shown in Table 2 and Table 3, respectively. In addition, the 5 most altered biological processes between the different experimental conditions have been compiled in Table 4. To this end, DEGs were identified via comparisons between the following cellular treatment conditions: 1) Zn-treatment *vs* control, 2) IL1α-treatment *vs* control, 3) Zn + IL1α-treatment *vs* control and 4) Zn + IL1α-treatment *vs* IL1α-treatment. No transcriptome data were obtained for the IL1α + Zn-treatment.

Zn-treatment vs control: The 24 h Zn-treatment had neither a significant effect on the entire gene expression profile of hfRPE cell cultures (data not shown), nor on the MT isoforms (see Table 2), when compared to control conditions. There was a slight increase in the expression of MT1E, MT1F and MT1G isoforms after Zn-treatment (fold-change = 1.7, with p-adj values < 0.05), but these expression differences were not statistically significant as in all cases the obtained fold-change was<2. The absence of an effect from Zn supplementation on the gene expression is striking, because the same Zn concentration (100 μM) and incubation time (24 h) previously exerted a systematic upregulation of the

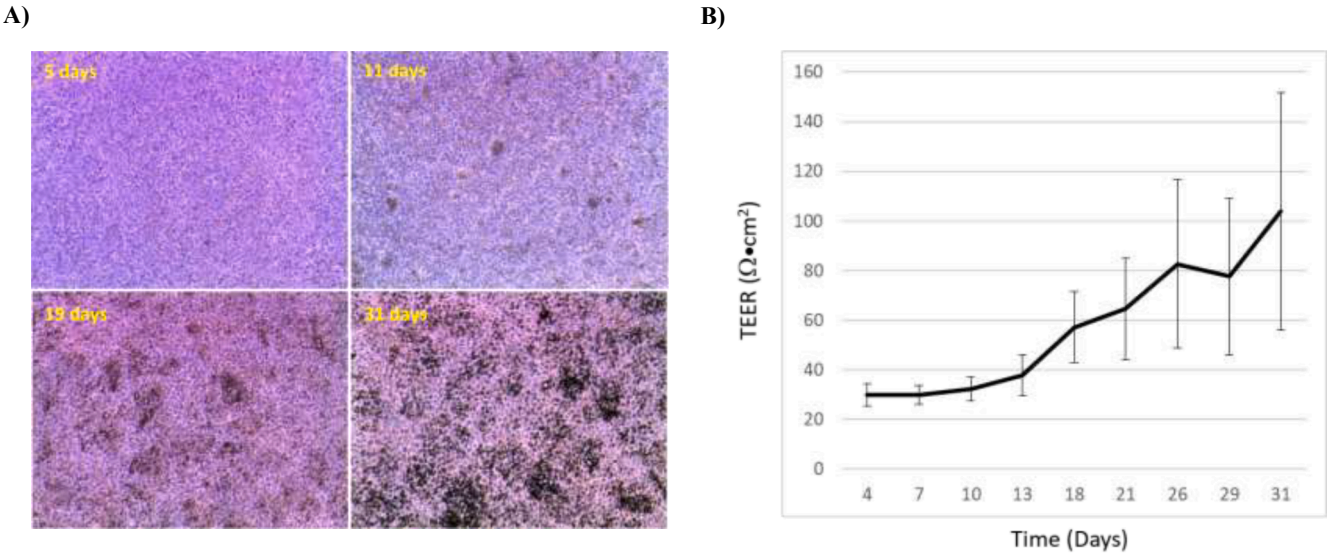

Fig. 2. A) Cobblestone morphology and pigmentation development over time. B) Mean value of TEER reached by the cultures over time.

Table 1
Canonical gene expression of RPE markers obtained for the samples from Plate 3. Expression levels are given as fragments per thousand bases of gene per million bases mapped (FPKM).

RPE markers	Control (FPKM)	Zn-treatment (FPKM)	IL1α-treatment (FPKM)	Zn + IL1α-treatment (FPKM)
BEST1	138	226	130	333
CRALBP	20	31	15	24
RPE65	8	16	9	15
RGR	17	29	41	81
TYR	256	260	196	259
MITF	62	64	58	63
TYRP1	2,101	2,144	1,797	2,242

gene expression of the MT isoforms in corneal (HCEsv) and lens (HLEsv) epithelial cell lines [32–34]. Moreover, upon exposure to the same Zn-treatment conditions, an *in vitro* model of human RPE (HRPEsv cell line) also responded with a significant increase in total MTs protein levels [41]. Probably, the optimal Zn-treatment conditions able to produce a response at the transcriptomic level in the hfRPE cell cultures are different than those previously assayed for immortalized human eye cell lines. In fact, matured RPE cells, with the observed tight junctions and characteristics of a functionally polarized monolayer, may respond in a less specific way to culture treatments, possible requiring a longer-term Zn treatment to see gene expression variations [40]. Along with MTs, other relevant molecules in Zn homeostasis are both ZnT (SLC30), and ZIP (SLC39) transporters, responsible for reducing and increasing the concentration of cytoplasmic Zn, respectively. Similarly, the gene expression of all ZnT and ZIP transporters remained unaltered during the Zn-treatment, when compared to control conditions, thus further suggesting that a longer Zn exposure is probably required for inducing alterations in Zn-related genes and transporters.

IL1α-treatment vs control: Likewise, upon exposure of primary hfRPE cells to IL1α, there were no statistically significant variations in MTs gene expression (see Table 2), similar as observed for the HCEsv cells [32] and in contrast to what happened in an HLEsv cell line [33], where there was an significant increase in their gene expression. Conversely, the 24 h IL1α-treatment induced statistically significant overexpression of the specific pro-inflammatory cytokines IL1α itself, IL1β and IL32. Moreover, overexpression of IL6 was also observed, which has both pro- and anti-inflammatory properties (Table 3). Additionally, IL1α-treatment induced a significant increase in complement factor B (CFB) (fold-change = 9.5, p-adj = 0) and complement C3 (fold-change = 17.3, p-adj = 0) gene expression, activating proteins playing a role within the alternative pathway of the complement system. The increased expression of both CFB and C3 could be, at least in part, mediated by IL6, the expression of which has been strongly induced by IL1α. It has been shown that IL6 induced increased levels of CFB and C3 at mRNA and protein levels in human skin fibroblast [42].

Also the increased gene expression of the Zn importer SLC39A8 (4.98 fold-change, p-adj = $1.04{\cdot}10^{-95}$) during pro-inflammatory conditions should be stressed. NF-κB (Nuclear Factor Kappa B) dependent upregulation of SLC39A8 expression, in response to TNFα (Tumor necrosis factor alpha) or LPS (lipopolysaccharide) was described earlier for primary human lung epithelia, monocytes and macrophages. In turn,

Table 2
Comparisons of gene expression for MTs isoforms between experimental conditions. Significant differences* correspond to an adjusted $p < 0.05$ and a fold change ≥ 2.0 or ≤ 0.5.

Gene symbol	Zn *vs* Control		IL1α *vs* Control		Zn-IL1α *vs* Control		Zn-IL1α *vs* IL1α	
	Fold-change	*p-adj*	Fold-change	*p-adj*	Fold-change	*p-adj*	Fold-change	*p-adj*
MT1E	1.75	$1.14{\cdot}10^{-9}$	1.33	0.2676	1.33	0.1914	1.14	0.5372
MT2A	1.07	0.9997	1.32	0.2811	1.13	0.9374	0.64	$1.16{\cdot}10^{-4}$
MT1X	1.43	0.0008	1.24	0.6678	1.25	0.6525	0.96	0.8432
MT1F	1.75	$1.95{\cdot}10^{-12}$	1.35	0.0874	1.38	0.1811	0.98	0.9559
MT1A	1.00	0.9997	0.99	0.9996	0.98	0.9437	0.34	0.5917
MT3	1.00	0.9997	1.14	0.5367	1.05	0.9419	0.46	0.2925
MT1M	1.04	0.9997	1.03	0.9996	1.05	0.8843	1.03	0.9796
MT1G	1.67	$3.99{\cdot}10^{-12}$	1.05	0.9471	1.19	0.3127	2.93	0.1902

Table 3
Comparisons of gene expression for cytokines between treatment conditions. Significant differences * correspond to an adjusted $p < 0.05$ and a fold-change ≥ 2.0 or ≤ 0.5.

Gene symbol	Zn *vs* Control		IL1α *vs* Control		Zn-IL1α *vs* Control		Zn-IL1α *vs* IL1α	
	Fold-change	*p-adj*	Fold-change	*p-adj*	Fold-change	*p-adj*	Fold-change	*p-adj*
IL1α	1.00	0.9997	*2.78	$*7.35{\cdot}10^{-14}$	1.76	0.0014	*0.33	$*3.36{\cdot}10^{-05}$
IL1β	1.00	0.9997	*2.54	$*3.44{\cdot}10^{-12}$	1.45	0.0258	*0.22	$*3.30{\cdot}10^{-06}$
IL6	1.04	0.9997	*16.79	$*1.95{\cdot}10^{-175}$	*9.79	$*2.63{\cdot}10^{-73}$	0.59	$1.34{\cdot}10^{-06}$
IL10	1.00	0.9997	0.99	0.9996	0.98	0.9413	0.69	0.8232
IL11	1.00	0.9997	1.43	0.0746	1.18	0.8435	0.65	0.1326
IL12A	0.97	0.9997	0.97	0.9996	0.87	0.8921	0.76	0.4776
IL16	1.00	0.9997	0.88	0.9996	1.06	0.9625	1.83	0.1124
IL18	0.86	0.9997	0.66	0.0001	0.72	0.0463	1.11	0.4186
IL32	1.02	0.9997	*6.24	$*5.89{\cdot}10^{-69}$	*6.03	$*1.74{\cdot}10^{-50}$	0.96	0.6852
TNF	1.00	0.9997	1.00	0.9996	1.09	0.7822	1.86	0.5610
TGFB1	1.03	0.9997	0.94	0.9996	0.83	0.2524	0.89	0.1744
TGFB2	0.94	0.9997	1.01	0.9996	0.94	0.9413	0.93	0.4016
TGFB3	0.83	0.5491	1.72	$1.00{\cdot}10^{-8}$	1.16	0.6216	0.65	$5.51{\cdot}10^{-05}$
TGFBI	0.89	0.8268	1.02	0.9996	0.98	0.9710	0.96	0.6808
IL1R1	0.95	0.9997	1.87	$2.95{\cdot}10^{-5}$	1.19	0.8081	*0.47	$*1.50{\cdot}10^{-04}$
IL18R1	1.00	0.9997	1.03	0.9996	1.08	0.8114	1.38	0.7551

Table 4
Five most altered biological processes between experimental conditions.

Comparison	Gene Ontology	Term	Corrected p-value
IL1α *vs* Control	GO:0002376	Immune system process	$4.88e^{-23}$
	GO:0006952	Defense response	$6.19e^{-23}$
	GO:0019221	Cytokine-mediated signaling pathway	$6.47e^{-23}$
	GO:0034097	Response to cytokine	$1.04e^{-20}$
	GO:0071345	Cellular response to cytokine stimulus	$8.83e^{-20}$
Zn-IL1α *vs* Control	GO:0006952	Defense response	$3.25e^{-25}$
	GO:0006955	Immune response	$2.47e^{-22}$
	GO:0019221	Cytokine-mediated signaling pathway	$6.32e^{-22}$
	GO:0034097	Response to cytokine	$2.06e^{-20}$
	GO:0051707	Response to other organism	$1.23e^{-19}$
Zn-IL1α *vs* IL1α	GO:0010469	Regulation of signaling receptor activity	$4.06e^{-05}$
	GO:0019221	Cytokine-mediated signaling pathway	$2.08e^{-04}$
	GO:0006954	Inflammatory response	$6.65e^{-04}$
	GO:0035234	Ectopic germ cell programmed cell death	$9.98e^{-04}$
	GO:0008284	Positive regulation of cell proliferation	$1.67e^{-03}$

SLC39A8 is a negative regulator of the NF-κB signalling pathway through zinc-mediated suppression of IKK (I Kappa B Kinase) [43].

Zn + IL1α-treatment vs control: No up-regulation of MTs gene expression was induced in hfRPE cells treated with IL1α after Zn-exposure (Table 2), again probably because the high Zn internalization in the matured RPE cultures, characterized by the polarized traffic of ions and metabolites across the monolayer, requires long-term culture supplementation, in contrast to the increased expression of MTs observed in simplified cellular models [32,34]. Only significant over-expression of the pro-inflammatory cytokine IL32 (6.03 fold-change, p-adj $= 2.63{\cdot}10^{-50}$), and of the pro- and anti-inflammatory IL6 (9.79 fold-change, p-adj $= 2.63{\cdot}10^{-73}$) was observed. Finally, the genes encoding the activation of proteins involved in the complementary alternative pathway, CFB and C3, and the Zn importer protein SLC39A8, also showed increased expression after IL1α-treatment of cultures previously treated with Zn (9.38 fold-change, p-adj $= 3.53{\cdot}10^{-178}$, 5.41 fold-change, p-adj $= 1.88{\cdot}10^{-94}$ and 3.39 fold-change, p-adj $= 7.22{\cdot}10^{-38}$, respectively).

Zn + IL1α-treatment vs IL1α-treatment: Interestingly, the comparison between Zn supplementation followed by the 24 h pro-inflammatory IL1α-treatment and the IL1α-treatment alone showed no significant changes in MTs gene expression but revealed that Zn supplementation induced a statistically significant attenuation of the inflammatory effects of IL1α. Hence, as shown Table 3, significant down-regulation of IL1α, IL1β and IL1R1 was observed, demonstrating the anti-inflammatory effects of Zn in cultured hfRPE cells. This effect was not previously observed in the ocular cell lines HCEsv and HLEsv [32,33]. Moreover, the pre-treatment of cells with Zn prevented IL1α-induced up-regulation of CFB and C3 gene expression (0.561 fold-change, p-adj $= 1.08{\cdot}10^{-14}$ and 0.578 fold-change, p-adj $= 3.82{\cdot}10^{-12}$, respectively) and consequently, the activation of the alternative complementary pathway. IL1α-treatment after Zn supplementation also did not induce an increase in SLC39A8 gene expression (0.67 fold-change, p-adj $= 5.98{\cdot}10^{-6}$). All together, these data point towards an anti-inflammatory effect exerted by Zn in hfRPE cells.

Gene Ontology analysis identified the most significantly altered biological processes (DEGs) between the different treatments performed (Table 4). No comparisons with Zn-supplementation are shown, since, as mentioned above, this specific treatment did not induce DEGs. As expected, upon IL1α treatment, the DEGs were mainly associated with biological processes related to the response to cytokines and the most significantly dysregulated process was "immune system process". Similarly, comparison of the Zn + IL1α-treatment with the control conditions showed that the defence and immune response biological processes were very significantly affected. Moreover, when the DEGs induced by Zn + IL1α-treatment were compared with those induced by IL1α alone, the third most altered biological process was "inflammatory response", supporting the possible attenuation of the inflammatory response towards IL1α due to the previous supplementation with Zn. More detailed results about the most altered biological processes between conditions are shown in Figures S1 and S2 of the Supplementary Material.

Inflammation is a protective process induced by cells to fight dangerous stimuli and restore normal homeostasis [44]. Neurodegenerative diseases, including Alzheimer's disease, Parkinson's disease,

amyotrophic lateral sclerosis, glaucoma and age-related macular degeneration (AMD), are associated with cell-mediated immune responses sharing neuroinflammatory features [45–47]. The immune-privilege of the retina and its RPE can be compromised during aging, which contributes to the onset of neurodegenerative eye diseases. Specifically, the chronic immune process in the RPE leads to uncontrolled inflammation, resulting in cell damage as a result of the production of neurotoxic factors [1,2,48]. In this vein, Zn is an essential element involved in important cellular processes, including inhibition of cytokine expression by blocking the dimerization of Stat3 (signal transducer and activator of transcription 3) proteins or activating NF-κB [49,50].

In this work, the use of an *in vitro* cell culture model representative of the human RPE and mimicking the gene expression profiling of the matured tissue permitted the study of the simultaneous effects of Zn and IL1α in the absence of immune T and B lymphocytes. Overall, transcriptomic data provided evidence of altered inflammatory pathways of the *in vitro* model of matured RPE cells, reflecting changes in molecular processes associated to altered immune system processes and the cellular response to cytokines. At RNA level, the pro-inflammatory cytokine IL1α strongly induced immune processes, defense response and cellular response to cytokine stimulus in a cell culture of matured RPE cells. In addition, although Zn supplementation during 24 h did not show evident gene expression alterations, the subsequent attenuation of inflammation supports the capability of RPE cells responding to cytokines and the consequent reduction of the inflammatory damage.

3.3. Zn levels in cultured RPE cells

The total Zn content in the cells, and the Zn concentrations in the apical and basal solutions from Plates 1 and 2 were determined by means of single-collector sector-field ICP-MS for each Transwell® insert used throughout the experiment. For the control conditions (Plate 1), after 24 h, the average Zn content was 55.8 ± 8.8 μg/L for the apical solution, 37.6 ± 3.3 μg/L for the basal solution and 88 ± 23 fg/cell. Similar values were obtained after IL1α-treatment (apical solution: 45.1 ± 8.8 μg/L; basal solution: 41.5 ± 3.6 μg/L; cells: 119 ± 43 fg/cell), whereas in the case of Zn-treatment, the cellular amount (260 ± 45 fg/cell) and, in particular, the basal Zn concentration (1400 ± 210 μg/L) were increased, which reflects enhanced Zn internalization and increased diffusion across the tight monolayer constituted by the matured RPE (due to Zn addition, the concentration in the apical solution reached 3410 ± 200 μg/L Zn). In addition, the Zn content was also measured in the wash solutions. The negligible concentrations thus obtained demonstrated actual internalization and diffusion of Zn across the cell monolayer and allows the possibility of adsorption to the cell culture to be discarded. In Plate 2, the average Zn content in cells was 126 ± 50 fg/cell, 221 ± 34 fg/cell and 164 ± 36 fg/cell in case of the control conditions (48 h), IL1α + Zn-treatment and Zn + IL1α-treatment, respectively. These values showed higher intracellular incorporation of Zn after pro-inflammatory stress (IL1α + Zn-treatment), whereas no difference in terms of Zn incorporation was appreciated when Zn treatment was performed before the pro-inflammatory process (with respect to the control cells).

In addition, the apical and basal Zn concentrations were also evaluated for Plate 2 after 24 h under control conditions (apical solution: 57.8 ± 9.7 μg/L; basal solution: 44.9 ± 5.8 μg/L), after IL1α-treatment (apical solution: 68.1 ± 8.1 μg/L; basal solution: 44.5 ± 4.6 μg/L) and after Zn supplementation (apical solution: 3860 ± 210 μg/L; basal solution: 1314 ± 66 μg/L), showing a good reproducibility between plates. In order to assess repeatability within plates, the Zn content was assessed in all control cell cultures. For the 4 wells used as controls in Plate 1, the Zn content was: 16.2 ng, 11.8 ng, 17.9 ng and 10.4 ng per 160,000 hfRPE cells per insert, respectively), showing decent repeatability. The same trend was observed for Plate 2.

In terms of mass balance, it is crucial to verify that the Zn content added to the Transwell® plates remains constant after 24 h. This means that the sum of the amounts of Zn added to apical solution after Zn-treatment (800 μL of 6423 μg/L, resulting in 5138 ng), the original content in Miller solution (1600 μL of 39.3 μg/L, resulting in 63 ng) and in the control cells (14 ng) should correspond to the sum of the Zn contents in the apical solution, basal solution and cell layer after 24 h treatment. The values thus obtained were 2730 ng, 2237 ng and 42 ng, respectively, showing a recovery of 96 %. These data indicate absence of Zn contamination and loss along the experiments.

3.4. Assessment of the experimental conditions for Zn isotopic analysis via MC-ICP-MS

Under the optimized conditions, the reproducibility between both experiments was also assessed in terms of isotope ratios. As previously mentioned, cell layer replicates from the same Transwell® plate were combined prior to target element isolation. The Zn isotope ratios thus obtained for the cell monolayer determined for controls in Plate 1 were −0.24 ‰ for δ^{66}Zn, −0.32 ‰ for δ^{67}Zn and −0.39 ‰ for δ^{68}Zn. In Plate 2, the Zn isotopic composition was −0.25 ‰ for δ^{66}Zn, −0.34 ‰ for δ^{67}Zn and −0.40 ‰ for δ^{68}Zn, showing a good reproducibility. Under these conditions, it was not possible to evaluate the repeatability within plates.

Direct removal of the cells by the addition of 14 M HNO_3 to the Transwell® inserts followed by transfer of the solution to a Savillex beaker for subsequent mineralization turned out to a better approach to achieve reliable Zn isotopic composition data than trypsinization followed by acid digestion. This assumption was confirmed by means of elemental and isotopic analysis carried out in a parallel experiment in which cells were trypsinized instead of being directly frozen. The values obtained after trypsinization clearly show irreproducibility between replicates. As an illustration, the δ^{66}Zn values as obtained after IL1α-treatment are reported. The δ^{66}Zn values in the apical compartments were 0.08 ± 0.02 ‰; 0.33 ± 0.01 ‰ and 0.34 ± 0.02 ‰, whereas values of 0.27 ± 0.04 ‰; 0.09 ± 0.02 ‰ and −0.05 ± 0.03 ‰ were obtained in the basal solutions.

For evaluation of the instrumental precision on the Zn isotope ratios, both internal and external precision were evaluated in dry plasma conditions (using solutions containing 20 μg/L Zn and 20 μg/L Cu). The external precision was determined as the standard deviation (SD) for 8 measurements of the in-house standard within a measurement session, thus resulting in 0.03 ‰ for δ^{66}Zn, 0.05 ‰ for δ^{67}Zn and 0.04 ‰ for δ^{68}Zn, whereas the internal precision was calculated considering the internal precision (2se, 45 cycles) of those 8 measurements of the in-house standard during the same measurement session and provided values of 0.03 ‰ for δ^{66}Zn, 0.07 ‰ for δ^{67}Zn and 0.04 ‰ for δ^{68}Zn, (Tables S1 and S2). Experimental precision related to the sample preparation procedure, including digestion and Zn isolation, was also assessed. The precision, expressed as the standard deviation (SD) on the isotopic composition of 3 replicates (in this case using the apical medium collected 24 h after Zn addition from three different Transwell® inserts) was evaluated within a measurement session, resulting in values of 0.02 ‰ for δ^{66}Zn, 0.04 ‰ δ^{67}Zn and 0.08 ‰ δ^{68}Zn. To estimate the expanded uncertainty, the precision related to sample preparation and measurement were combined (see Table S1 and Table S2). A coverage factor k = 2 was used, resulting in an expanded uncertainty of 0.08 ‰ for δ^{66}Zn, 0.15 ‰ for δ^{67}Zn and 0.18 ‰ for δ^{68}Zn. Moreover, the average Zn isotope ratio results and corresponding standard deviations for the in-house standard (measured 68 times during 10 different sessions) were also reported, resulting in −7.00 ± 0.09 ‰ (2SD) for δ^{66}Zn, −10.43 ± 0.16 ‰ for δ^{67}Zn and −13.85 ± 0.14 ‰ for δ^{68}Zn. The standard deviations thus obtained show the reproducibility of the measurement values. The δZn values obtained also nicely plot on a mass-dependent fractionation line, further demonstrating reliability of the data. In addition, the δ^{66}Zn ± 2se values obtained for the in-house standard replicates determined within each measurement session and the mean value ± 2SD for n replicates measured in each session, are also indicated (Fig. S3).

The instrumental precision on the Zn isotope ratios was also assessed under wet plasma conditions (using a solution containing 200 μg/L of Zn and 200 μg/L of Cu). The internal precision thus obtained was 0.02 ‰ for δ^{66}Zn, 0.04 ‰ for δ^{67}Zn and 0.03 ‰ for δ^{68}Zn, whereas the external precision was 0.02 ‰ for δ^{66}Zn, 0.05 ‰ for δ^{67}Zn and 0.02 ‰ for δ^{68}Zn. Moreover, the average Zn isotope ratio data and standard deviations for the in-house standard (measured 25 times during 3 different sessions) was −7.04 ± 0.05 ‰ for δ^{66}Zn, −10.50 ± 0.11 ‰ for δ^{67}Zn and −13.92 ± 0.09 ‰ for δ^{68}Zn, in excellent agreement with previously published results (-7.03 ± 0.05 ‰ for δ^{66}Zn, −10.50 ± 0.21 ‰ for δ^{67}Zn and −13.90 ± 0.20 ‰ for δ^{68}Zn) [51].

3.5. Zn isotopic analysis in primary RPE cell cultures by MC-ICP-MS

Alterations in the Zn isotopic composition caused by inflammation induced in a mature RPE cell culture forming a monolayer that mimics native tissue were investigated. Also, protective effects associated to Zn have been assessed via short-term Zn supplementation.

Fig. 3 shows the isotopic composition, expressed as δ^{66}Zn (‰) for the apical solution, basal solution and cells after incubation in a) Miller medium for 24 h (control 24 h), b) IL1α for 24 h, c) 100 μM Zn for 24 h, d) Miller medium for 48 h (control 48 h), e) IL1α for 24 h followed by 100 μM Zn for another 24 h, and f) 100 μM Zn for 24 h followed by IL1α for another 24 h. Results obtained for δ^{66}Zn, δ^{67}Zn and δ^{68}Zn (‰), have been gathered in Table 5. Panels A and D (Fig. 3) show the isotopic composition of Zn in control conditions (*i.e.*, Miller medium) at 24 h and 48 h, respectively, in both the apical and basal compartment, as well as the Zn isotopic composition measured in the cells. It can be seen that a similar Zn isotopic composition was found when comparing the results for the apical compartments at 24 h and 48 h and for the basal compartments at 24 h and 48 h. Furthermore, a similar isotopic composition was reported for the apical and basal sides at 24 h (Panel A) and for the apical and basal compartments in Panel D. However, the cellular Zn composition showed a lighter isotopic composition of −0.24 (‰) and −0.25 (‰) at 24 h and 48 h, respectively, which is significantly different from that of the culture Miller medium (0.58 ± 0.02 ‰). It can be also seen that the Zn isotopic composition measured in the apical and basal media after Zn supplementation (Panel C) or after Zn following IL1α treatment (Panel E) is similar to that measured in the Zn-supplemented Miller solution (−0.15 ± 0.03 ‰), evidencing a high diffusion of Zn throughout the RPE monolayer. However, when Zn-supplementation is performed before the IL1 α treatment, the Zn isotopic compositions found in apical and basal media were 0.15 ± 0.04 ‰ and −0.02 ± 0.09 ‰, respectively (0.43 ± 0.01 ‰ was measured in IL1 α solution). Mass balance in this last case reflected that probably some Miller medium from the Zn supplementation was left in the Transwell® before adding the IL1 α, being 266 ng Zn more as compared to added Zn and therefore affect the isotopic composition of apical and basal media when the IL1 α treatment is performed. Still, when considering contribution of the remanent solution in both sides of the Transwell® results obtained evidence a trend towards a lighter Zn isotopic composition in the basal compartment with respect to the apical one. Last, when comparing Panel B (IL1 α treatment) and Panel F (Zn + IL1 α treatment), the δ^{66}Zn values found in the basal and apical media were different, with the δ^{66}Zn values similar to those found in the media added at the basal and apical sides of the Transwell® inserts.

For isotope ratio measurements in the cultured cells, it should be accounted first that the Zn isotopic composition in the control cells (Panel A: −0.24 ± 0.03 ‰ & Panel D: −0.25 ± 0.03 ‰) was similar to that of the Zn used for supplementation, *i.e.* −0.15 ± 0.03 ‰. Therefore, detection of variations in the isotopic composition of Zn in the cells as a consequence of supplementation is hindered. Nevertheless, when comparing the Zn isotopic composition in the control cells to those for the IL1α treatment (Panel B) and IL1α treatment followed by Zn-supplementation (Panel E), differences can be observed. In particular, despite the IL1 α medium is enriched in the heavier isotopes, after 24 h

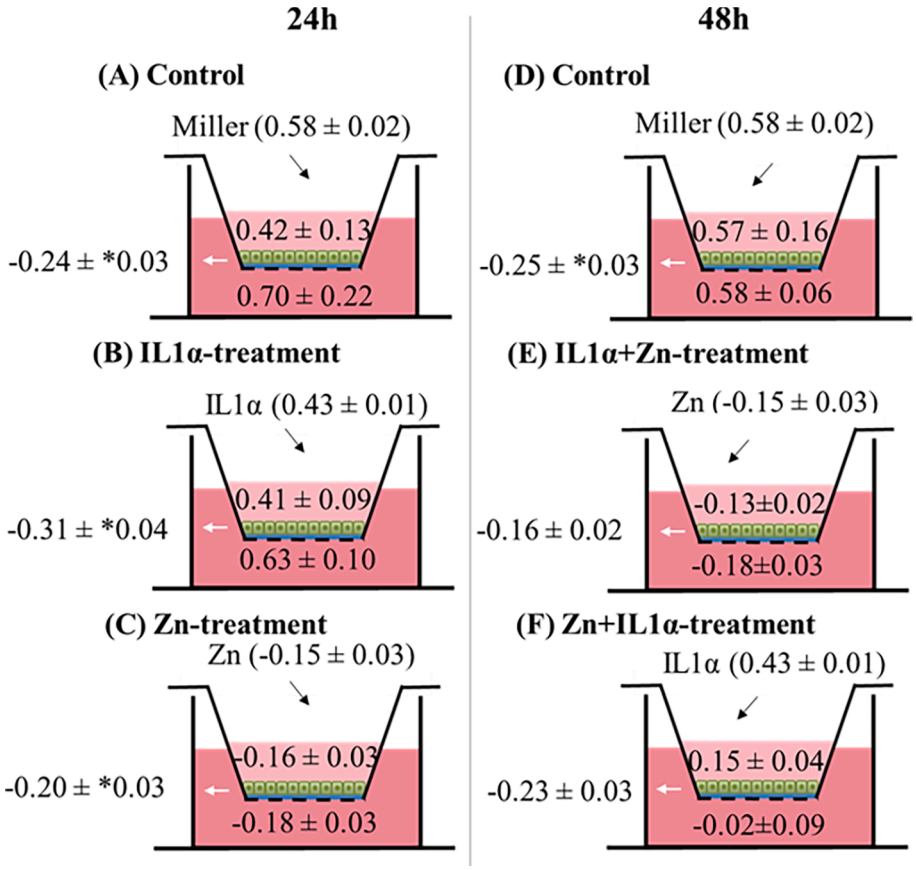

Fig. 3. δ^{66}Zn values (expressed in ‰) in cells, apical and basal solutions for A) control at 24 h, B) IL1α-treatment, C) Zn-treatment, D) control at 48 h, E) IL1α + Zn-treatment and F) Zn + IL-1α-treatment. Uncertainties, calculated whenever possible, were expressed as the standard deviation (SD) of the measurement replicates. For those cases without sample replicates, as a result of their combination for the isotope ratio measurements due to the low amount of Zn (cells A-D), the SD (indicated with *) was determined based on the relative standard deviation (RSD) for the cells replicates (cells E and F).

Table 5
Zn isotope ratio results, expressed as δ^{66}Zn, δ^{67}Zn and δ^{68}Zn (‰) in the cells, apical, basal and media solutions throughout the experiments detailed in Fig. 1. Uncertainties are expressed as the standard deviation (SD) of the measurement replicates. For those cases without sample replicates (as a result of their combination for the isotope ratio measurements due to the low amount of Zn), the SD (indicated with *) was determined based on the relative standard deviation (RSD) of the cells replicates.

24 h (Plate 1)	Control (24 h)			IL1α-treatment			Zn-treatment		
Compartment	δ^{66}Zn (‰)	δ^{67}Zn (‰)	δ^{68}Zn (‰)	δ^{66}Zn (‰)	δ^{67}Zn (‰)	δ^{68}Zn (‰)	δ^{66}Zn (‰)	δ^{67}Zn (‰)	δ^{68}Zn (‰)
Apical	0.42 ± 0.13	0.58 ± 0.17	0.85 ± 0.24	0.41 ± 0.09	0.59 ± 0.10	0.81 ± 0.15	−0.16 ± 0.03	−0.23 ± 0.05	−0.33 ± 0.04
Cells	−0.24 ± *0.03	−0.32 ± *0.03	−0.39 ± *0.05	−0.31 ± *0.04	−0.36 ± *0.03	−0.56 ± *0.07	−0.20 ± *0.03	−0.34 ± *0.03	−0.38 ± *0.05
Basal	0.70 ± 0.22	0.98 ± 0.22	1.34 ± 0.37	0.63 ± 0.10	1.09 ± 0.19	1.27 ± 0.23	−0.18 ± 0.03	−0.28 ± 0.05	−0.36 ± 0.04
48 h (Plate 2)	**Control (48 h)**			**IL1α + Zn-treatment**			**Zn + IL1α-treatment**		
Compartment	**δ^{66}Zn (‰)**	**δ^{67}Zn (‰)**	**δ^{68}Zn (‰)**	**δ^{66}Zn (‰)**	**δ^{67}Zn (‰)**	**δ^{68}Zn (‰)**	**δ^{66}Zn (‰)**	**δ^{67}Zn (‰)**	**δ^{68}Zn (‰)**
Apical	0.57 ± 0.16	1.05 ± 0.39	1.13 ± 0.26	−0.13 ± 0.02	−0.24 ± 0.03	−0.29 ± 0.03	0.15 ± 0.04	0.20 ± 0.07	0.36 ± 0.06
Cells	−0.25 ±*0.03	−0.34 ± *0.03	−0.40 ± *0.05	−0.16 ± 0.02	−0.15 ± 0.07	−0.30 ± 0.02	−0.23 ± 0.03	−0.34 ± 0.03	−0.44 ± 0.06
Basal	0.58 ± 0.06	0.96 ± 0.19	1.14 ± 0.07	−0.18 ± 0.03	−0.25 ± 0.05	−0.35 ± 0.05	−0.02 ± 0.09	0.03 ± 0.09	0.03 ± 0.08
Isotopic composition of media	**Miller Medium**			**100 U/mL IL1α in Miller medium**			**100 μM Zn in Miller medium**		
	δ^{66}Zn (‰)	**δ^{67}Zn (‰)**	**δ^{68}Zn (‰)**	**δ^{66}Zn (‰)**	**δ^{67}Zn (‰)**	**δ^{68}Zn (‰)**	**δ^{66}Zn (‰)**	**δ^{67}Zn (‰)**	**δ^{68}Zn (‰)**
	0.58 ± 0.02	0.92 ± 0.08	1.17 ± 0.03	0.43 ± 0.01	0.63 ± 0.09	0.77 ± 0.05	−0.15 ± 0.03	−0.29 ± 0.01	−0.34 ± 0.03

of treatment, the Zn isotopic composition in the cells shifted in favour of the lighter isotopes in comparison to control cells. Also, the Zn isotopic composition in the cells after 48 h of treatment (Panel E) was equal to that of the Zn-supplemented Miller solution, thus probably due to the higher intracellular incorporation of Zn after pro-inflammatory stress (Panel B: 19.0 ± 6.8 ng & Panel E: 35.3 ± 5.4 ng).

4. Conclusions

We demonstrated, at RNA level, that the *in vitro* model of RPE strongly responded to pro-inflammatory events by inducing immune and cytokine responses, while Zn supplementation was able to partially attenuate the inflammatory effects thus prompted. Interestingly, the established RPE model also showed changes in the isotopic composition of Zn with a cellular enrichment in the lighter isotopes, indicating altered homeostasis during inflammation, which has been partially compensated for via short-term zinc supplementation, probably indicating modulation of the cellular immune function via cytokine signaling. Although IL1α triggered the expression of pro-inflammatory cytokines and SLC39A8 Zn importer, and lighter intracellular Zn isotopic compositions were observed, there is no evidence for Zn uptake into or release from the intracellular space.

5. Data availability

All data generated or analyzed during this study are included in this article and supplementary information files. Additionally, RNA sequences data have been deposited in ArrayExpress database under accession number E-MTAB-11891.

Declaration of Competing Interest

The authors declare that they have no known competing financial interests or personal relationships that could have appeared to influence the work reported in this paper.

Acknowledgments

This work was financially supported through project PID2019-107838RB-I00/Agencia Estatal de Investigación (AEI)/10.13039/501100011033) in Spain. M.A. acknowledges the University of Oviedo for the Ph.D. grant ref. PAPI-21-PF-05. F.V acknowledges the Flemish Research Foundation (FWO) for providing the funding for the acquisition of the MC-ICP-MS instrumentation (ZW15-02 – G0H6216N). M.C.R. thanks FWO for her senior postdoctoral grant.

Author contributions

M.A. carried out the elemental assay and isotopic analysis experiments and drafted the first version of the manuscript; A.A.B. was responsible for the treatments applied to the cells; M.C.R. participated in the design and measurements of the elemental assay and isotopic analysis experiments and drafting of the manuscript; L.L. participated in the design of the experiments to be applied to the cells and drafting of the manuscript; L.A. has grown the cells prior to applying the different treatments and was responsible for the transcriptome analysis; H.G.I. participated in the design of the cell experiments and revision of the manuscript; R.P. carried out a final revision of the manuscript on behalf of the group at the University of Oviedo and F.V. carried out a final revision of the manuscript on behalf of the group at Ghent University.

Appendix A. Supplementary data

Supplementary data to this article can be found online at https://doi.org/10.1016/j.microc.2022.108033.

References

[1] A. Kauppinen, J.J. Paterno, J. Blasiak, A. Salminen, K. Kaarniranta, Inflammation and its role in age-related macular degeneration, Cell Mol. Life Sci. 73 (2016) 1765–1786, https://doi.org/10.1007/s00018-016-2147-8.

[2] E. Buschini, A. Piras, R. Nuzzi, A. Vercelli, Age related macular degeneration and drusen: neuroinflammation in the retina, Prog. Neurobiol. 95 (2011) 14–25, https://doi.org/10.1016/j.pneurobio.2011.05.011.

[3] P. Wang, D. Zhou, Y. Liao, J. Wu, A new peptide-based fluorescent probe for highly selective and sensitive detection of zinc (II) and application in real samples and cells imaging, Microchem. J. 161 (2021), 105760, https://doi.org/10.1016/j.microc.2020.105760.

[4] J. Liu, L. Zheng, X. Wei, B. Wang, H. Chen, M. Chen, M. Wang, W. Feng, J. Wang, Quantitative imaging of trace elements in brain sections of Alzheimer's disease mice with laser ablation inductively coupled plasma-mass spectrometry, Microchem. J. 172 (2022), 106912, https://doi.org/10.1016/j.microc.2021.106912.

[5] K.W. Leung, M. Liu, X. Xu, M.J. Seiler, C.J. Barnstable, J. Tombran-Tink, Expression of ZnT and ZIP zinc transporters in the human RPE and their regulation by neurotrophic factors, IOVS 49 (2008) 1221–1230, https://doi.org/10.1167/iovs.07-0781.

[6] A.S. Prasad, Zinc: role in immunity, oxidative stress and chronic inflammation, Curr. Opin. Clin. Nutr. Metab. Care 12 (2009) 646–652, https://doi.org/10.1097/MCO.0b013e3283312956.

[7] R. Gilbert, T. Peto, I. Lengyel, E. Emri, Zinc nutrition and Inflammation in the Aging Retina, Mol. Nutr. Food Res. 63 (15) (2019) 1801049.

[8] H. Haase, L. Rink, The immune system and the impact of zinc during aging, Immunity Aging 6 (2009) 17, https://doi.org/10.1186/1742-4933-6-9.

[9] Age-Related Eye Disease Study Researh Group, A randomized placebo-controlled, clinical trial of high-dose supplementation with vitamins C and E, beta carotene, and zinc for age-related macular degeneration and vision loss: AREDS report no.8, Arch. Ophthalmol. 119 (2001) 1417-1436. doi:10.1001/archopht.119.10.1417.

[10] B.L. Vallee, K.H. Falchuck, The biochemical basis of zinc physiology, Physiol. Rev. 73 (1993) 79–118, https://doi.org/10.1152/physrev.1993.73.1.79.

[11] M. Ugarte, N.N. Osborne, L.A. Brown, P.N. Bishop, Iron, zinc and copper in retinal physiology and disease, Surv. Ophthalmol. 58 (2013) 585–609, https://doi.org/10.1016/j.survophthal.2012.12.002.

[12] A. Varin, A. Larbi, G.V. Dedoussis, S. Kanoni, J. Jajte, L. Rink, D. Monti, M. Malavolta, F. Marcellini, E. Mocchegiani, G. Herbein, T. Fulop, In vitro and in vivo effects of zinc on cytokine signalling in human T cells, Exp. Gerontol. 43 (5) (2008) 472–482.

[13] L. Kahmann, P. Uciechowski, S. Warmuth, B. Plümäkers, A.M. Gressner, M. Malavolta, E. Mocchegiani, L. Rink, Zinc supplementation in the elderly reduces spontaneous inflammatory cytokine release and restores T cell functions, Rejuvenation Res. 11 (2008) 227–237, https://doi.org/10.1089/rej.2007.0613.

[14] R.A. Colvin, W.R. Holmes, C.P. Fontaine, W. Maret, Cytosolic zinc buffering and muffling. Their role in intracellular zinc homeostasis, Metallomics 2 (2019) 306–317, https://doi.org/10.1039/b926662c.

[15] L. Álvarez, H. González-Iglesias, M. García, S. Ghosh, A. Sanz-Medel, M. Coca-Prados, The stoichiometric transition from Zn6Cu1-Metallothionein to Zn7-Metallothionein underlies the up-regulation of metallothionein (MT) expression, J. Bio. Chem. 287 (2012) 28456–28469, https://doi.org/10.1074/jbc.M112.365015.

[16] F. Vanhaecke, M. Costas-Rodríguez, High-precision isotopic analysis of essential mineral elements: capabilities as a diagnostic/prognostic tool, View 2 (2021) 20200094, https://doi.org/10.1002/VIW.20200094.

[17] F. Vanhaecke, L. Balcaen, D. Malinovski, Use of single-collector and multi-collector ICP-mass spectrometry for isotopic analysis, J. Anal. At. Spectrom. 24 (2009) 863–886, https://doi.org/10.1039/B903887F.

[18] F. Albarede, P. Telouk, A. Lamboux, K. Jaouen, V. Balter, Isotopic evidence of unaccounted for Fe and Cu eythropoietic pathways, Metallomics 3 (2011) 926–933, https://doi.org/10.1039/c1mt00025j.

[19] M. Costas-Rodríguez, Y. Anoshkina, S. Lauwens, H. Van Vlierberghe, J. Delanghe, F. Vanhaecke, Isotopic analysis of Cu in blood serum by multicollector ICP-mass spectrometry: a new approach for the diagnosis and prognosis of liver cirrhosis, Metallomics 7 (2015) 491–498, https://doi.org/10.1039/c4mt00319e.

[20] M. Aramendia, L. Rello, M. Resano, F. Vanhaecke, Isotopic anlaysis of Cu in serum samples for diagnosis of Wilsoń disease: a pilot study, J. Anal. At. Spectrom. 28 (2013) 675–681, https://doi.org/10.1039/C3JA30349G.

[21] M. Aranaz, M. Costas-Rodríguez, L. Lobo, M. García, H. González-Iglesias, R. Pereiro, F. Vanhaecke, Homeostatic alterations related to total antioxidant capacity, elemental concentrations and isotopic compositions in aqueous humor of glaucoma patients, Anal. Bioanal. Chem. 414 (1) (2022) 515–524, https://doi.org/10.1007/s00216-021-03467-5.

[22] F. Larner, L.N. Woodley, S. Shousha, A. Moyes, E. Humphreys-Williams, S. Strekopytov, A.N. Hallida, M. Rehkamper, R.C. Coombes, Zinc isotopic compositions of breast cancer tissue, Metallomics 7 (2015) 112–117, https://doi.org/10.1039/c4mt00260a.

[23] K. Schilling, R.E.T. Moore, K.V. Sullivan, M.S. Capper, M. Rehkämper, K. Goddard, C. Ion, R.C. Coombes, L. Vesty-Edwards, A.D. Lamb, A.N. Halliday, F. Larner, Zinc stable isotopes in urine as diagnostic for cancer of secretory organs, Metallomics 13 (2021) mfab020, https://doi.org/10.1093/mtomcs/mfab020.

[24] M.R. Flórez, Y. Anoskina, M. Costas-Rodríguez, C. Grootaert, J. Van Camp, J. Delanghe, F. Vanhaecke, Natural Fe isotope fractionation in an intestinal Caco-2 cell line model, J. Anal. At. Spectrom. 32 (2017) 1713–1720, https://doi.org/10.1039/C7JA00090A.

[25] V.P. Bondanese, A. Lamboux, M. Simon, J.E. Lafont, E. Albalat, S. Pichat, J. Vanacker, P. Telouk, V. Balter, P. Oger, F. Albarède, Hypoxia induces copper stable isotope fractionation in hepatocellular carcinoma, in a HIF-independent manner, Metallomics 8 (2016) 1177–1184, https://doi.org/10.1039/c6mt00102e.

[26] M.R. Flórez, M. Costas-Rodríguez, C. Grootaert, J. Van Camp, F. Vanhaecke, Cu isotope fractionation response to oxidative stress in a hepatic cell line studied using multi-collector ICP-mass spectrometry, Anal. Bioanal. Chem. 410 (2018) 2385–2394, https://doi.org/10.1007/s00216-018-0909-x.

[27] E. Paredes, E. Avazeri, V. Malard, C. Vidaud, P.E. Reiller, R. Ortega, A. Nonell, H. Isnard, F. Chartier, C. Bresson, Evidence of isotopic fractionation of natural uranium in cultured human cells, Proc. Natl. Acad. Sci. 113 (2016) 14007–14012, https://doi.org/10.1073/pnas.1610885113.

[28] M. Costas-Rodríguez, L. Colina-Vegas, N. Solovyev, O. De Wever, F. Vanhaecke, Cellular and sub-cellular Cu isotope fractionation in the human neuroblastoma SH-SY5Y cell line: proliferating versus neuron-like cells, Anal. Bioanal. Chem. 411 (2019) 4963–4971, https://doi.org/10.1007/s00216-019-01871-6.

[29] K. Schilling, A.L. Harris, A.N. Halliday, C.J. Schofield, H. Sheldon, S. Haider, F. Larner, Investigations on zinc isotope fractionation in breast cancer tissue using in vitro cell culture uptake-efflux experiments, Front. Med. 8 (2022), 746532, https://doi.org/10.3389/fmed.2021.746532.

[30] A. Maminishkis, S. Chen, S. Jalickee, T. Banzon, G. Shi, F.E. Wang, T. Ehalt, J. A. Hammer, S.S. Miller, Confluent monolayers of cultured human fetal retinal pigment epithelium exhibit 24 morphology and physiology of native tissue, Investig. Ophthalmol. Vis. Sci. 47 (2006) 3612–3624, https://doi.org/10.1167/iovs.05-1622.

[31] B. Srinivasan, A.R. Kolli, M.B. Esch, H.E. Abaci, M.L. Shuler, J.J. Hickman, TEER measurement techniques for in vitro barrier model systems, J. Lab. Autom. 20 (2015) 107–126, https://doi.org/10.1177/2211068214561025.

[32] H. Gonzalez Iglesias, C. Petrash, S.M. Rodríguez-Menéndez, M. Garcia, L. Alvarez, L. Fernández-Vega Cueto, B. Fernández, R. Pereiro, A. Sanz-Medel, M. Coca-Prados, Quantitative distribution of Zn, Fe and Cu in the human lens and study of the Zn metallothionein redox system in cultured lens epithelial cells by elemental MS, J. Anal. At. Spectrom. 32 (2017) 1746–1756, https://doi.org/10.1039/C6JA00431H.

[33] S. Rodríguez-Menéndez, B. Fernández, M. García, L. Álvarez, M.L. Fernández, A. Sanz-Medel, M. Coca-Prados, R. Pereiro, H. González-Iglesias, Quantitative study of zinc and metallothioneins in the human retina and RPE cells by mass spectrometry-based methodologies, Talanta 178 (2018) 222–230, https://doi.org/10.1016/j.talanta.2017.09.024.

[34] M.I. Love, W. Huber, S. Anders, Moderated estimation of fold change and dispersion for RNA-seq data with DESeq2, Genome Biol. 15 (2014) 550, https://doi.org/10.1186/s13059-014-0550-8.

[35] Bioconductor, Open source software for bioinformatics http://www.bioconductor.org/packages/release/bioc/html/DESeq2.html (last access 30 June 2022).

[36] S. Lauwens, M. Costas-Rodriguez, H. Van Vlierberghe, F. Vanhaecke, Cu isotopic signature in 573 blood serum of liver transplant patients: a follow-up study, Sci. Rep. 6 (2016) 30683, https://doi.org/10.1038/srep30683.

[37] D.C. Baxter, I. Rodushkin, E. Engström, D. Malinovsky, Revised exponential model for mass bias correction using an internal standard for isotope abundance ratio measurements by multi-collector inductively coupled plasma mass spectrometry, J. Anal. At. Spectrom. 21 (4) (2006) 427.

[38] M.G. Pilgrim, I. Lengyel, A. Lanzirotti, M. Newville, S. Fearn, E. Emri, J.C. Knowles, J.D. Messinger, R.W. Read, C. Guidry, C.A. Curcio, Subretinal Pigment Epithelial Deposition of Drusen Components Including Hydroxyapatite in a Primary Cell Culture Model, Invest. Ophthalmol. Vis. Sci. 58 (2017) 708–719, https://doi.org/10.1167/iovs.16-21060.

[39] P.J. Pao, E. Emri, S.B. Abdirahman, T. Soorma, H.H. Zeng, S.M. Hauck, R. B. Thompson, I. Lengyel, The effects of zinc supplementation on primary human retinal pigment epithelium, J. Trace Elem. Med. Biol. 49 (2018) 184–191, https://doi.org/10.1016/j.jtemb.2018.02.028.

[40] E. Emri, E. Kortvely, S. Dammeier, F. Klose, D. Simpson, EYE.-R. Consortium, A. I. den Hollander, M. Ueffing, I. Lengyel, A Multi-Omics Approach Identifies Key Regulatory Pathways Induced by Long-Term Zinc Supplementation in Human Primary Retinal Pigment Epithelium, Nutrients 12 (10) (2020) 3051.

[41] S. Rodríguez-Menéndez, M. García, B. Fernández, L. Álvarez, A. Fernández-Vega-Cueto, M. Coca-Prados, R. Pereiro, H. González-Iglesias, The Zinc-Metallothionein Redox System Reduces Oxidative Stress in Retinal Pigment Epithelial Cells, Nutrients 10 (2018) 1874, https://doi.org/10.3390/nu10121874.

[42] Y. Katz, M. Revel, R.C. Strunk, Interleukin 6 stimulates synthesis of complement proteins factor B and C3 in human skin fibroblasts, Eur. J. Immunol. 19 (1989) 983–988, https://doi.org/10.1002/eji.1830190605.

[43] M. Liu, S. Bao, M. Gálvez-Peralta, C.J. Pyle, A.C. Rudawsky, R.E. Pavlovicz, D. W. Killilea, C. Li, D.W. Nebert, M.D. Wewers, D.L. Knoell, ZIP8 regulates host defense through zinc-mediated inhibition of NF-κB, Cell Rep. 3 (2013) 386–400, https://doi.org/10.1016/j.celrep.2013.01.009.

[44] C.K. Glass, K. Saijo, B. Winner, M.C. Marchetto, F.H. Gage, Mechanisms underlying inflammation in neurodegeneration, Cell 140 (2010) 918–934, https://doi.org/10.1016/j.cell.2010.02.016.

[45] M.L. Block, J.S. Hong, Microglia and inflammation-mediated neurodegeneration: multiple triggers with a common mechanism, Prog. Neurobiol. 76 (2005) 77–98, https://doi.org/10.1016/j.pneurobio.2005.06.004.

[46] D.H. Anderson, R.F. Mullins, G.S. Hageman, L.V. Johnson, A role for local inflammation in the formation of drusen in the aging eye, Am. J. Ophthalmol. 134 (2002) 411–431, https://doi.org/10.1016/s0002-9394(02)01624-0.

[47] M.B. Wax, G. Tezel, Immunoregulation of retinal ganglion cell fate in glaucoma, Exp. Eye Res. 88 (2009) 825–830, https://doi.org/10.1016/j.exer.2009.02.005.

[48] M. Chen, C. Luo, J. Zhao, G. Devarajan, H. Xu, Immune regulation in the aging retina, Prog. Retin. Eye Res. 69 (2019) 159–172, https://doi.org/10.1016/j.preteyeres.2018.10.003.
[49] C. Kitabayashi, T. Fukada, M. Kanamoto, W. Ohashi, S. Hojyo, T. Atsumi, N. Ueda, I. Azuma, H. Hirota, M. Murakami, T. Hirano, Zinc suppresses Th17 development via inhibition of STAT3 activation, Int. Immunol. 22 (2010) 375–386, https://doi.org/10.1093/intimm/dxq017.
[50] P. Bonaventura, G. Benedetti, F. Albarède, P. Miossec, Zinc and its role in immunity and inflammation, Autoimmun. Rev. 14 (2015) 277–285, https://doi.org/10.1016/j.autrev.2014.11.008.
[51] L. Van Heghe, E. Engström, I. Rodushkin, C. Cloquet, F. Vanhaecke, Isotopic analysis of the metabolically relevant transition metals Cu, Fe and Zn in human blood from vegetarians and omnivores using multi-collector ICP-mass spectrometry, J. Anal. At. Spectrom. 27 (2012) 1327–1334, https://doi.org/10.1039/C2JA30070B.